Comparative Analysis of UAS Photogrammetric Accuracy: Influence of Flight Altitude on Accuracy and Operational Efficiency in Urban Mapping

Emanuel Amorim[1], Diogo Inojosa[2], Jailson Rodrigues Júnior[3], Eveliny Matias[4], Leandro França[5] Simone Sato[6]

[1] Dept. of Cartographic Engineering, Federal University of Pernambuco (UFPE), Recife, Brazil – emanuel.rramorim@ufpe.br
[2] Dept. of Cartographic Engineering, Federal University of Pernambuco (UFPE), Recife, Brazil – diogo.finojosa@ufpe.br
[3] Dept. of Cartographic Engineering, Federal University of Pernambuco (UFPE), Recife, Brazil – jailson.rodriguesjunior@ufpe.br
[4] Dept. of Cartographic Engineering, Federal University of Pernambuco (UFPE), Recife, Brazil – eveliny.matias@ufpe.br
[5] Dept. of Civil Engineering, Federal University of Pernambuco (UFPE), Recife, Brazil – leandro.silvafranca@ufpe.br
[6] Dept. of Cartographic Engineering, Federal University of Pernambuco (UFPE), Recife, Brazil – simone.sato@ufpe.br

Keywords: GSD; efficiency; GNSS; Ntrip; Agisoft Metashape; Flight Height

Abstract

UAS photogrammetry has become an efficient solution for acquiring high-resolution geospatial data for urban mapping, environmental monitoring, and 3D modelling. However, mission planning still involves a trade-off between data quality and operational efficiency, particularly regarding flight altitude, which directly affects ground sample distance (GSD), point cloud density, and positional accuracy. This study evaluates the influence of flight altitude through a controlled comparison of two urban photogrammetric surveys: a low-altitude flight at 61.2 m (GSD = 1.56 cm/pix, 420 images) and a higher-altitude flight at 121 m (GSD = 3.11 cm/pix, 116 images). Both surveys used RGB cameras with equivalent image resolution mounted on different platforms, which constitutes an experimental limitation, while overlap and processing parameters were kept constant. The results show that the lower-altitude flight produced denser data and better geometric performance, with lower reprojection error and lower check point RMSE. In contrast, the higher-altitude flight provided greater operational efficiency, covering a larger area with fewer images and lower computational demand. These findings indicate that both strategies are technically viable but suited to different objectives: lower altitudes favour geometric detail and positional accuracy, whereas higher altitudes improve productivity and area coverage. Therefore, flight altitude should be selected according to project requirements, balancing geometric quality and operational efficiency.

1. Introduction

With the advancement of sensors, platforms, and processing workflows based on Structure from Motion (SfM) and Multi-View Stereo (MVS), photogrammetry using Unmanned Aerial Systems (UAS) in digital photogrammetry has become established as an efficient alternative for the acquisition of high-resolution geospatial data. Its application has been expanding in urban mapping, three-dimensional modeling, cadastre, inspection, environmental monitoring (Gomes et al., 2024), infrastructure monitoring, disaster response, precision agriculture, and archaeological documentation, mainly due to the combination of operational flexibility, rapid data acquisition, and the potential to generate metric products with centimeter-level resolution (Niu et al., 2024).

In this context, flight planning plays a decisive role in the geometric quality of photogrammetric products. Parameters such as flight altitude, longitudinal and lateral overlap, acquisition geometry, distribution of control points, and georeferencing strategy directly influence the Ground Sample Distance (GSD), point cloud density, bundle adjustment stability, and the positional accuracy of the generated models. Recent studies have shown that final quality depends not only on spatial resolution, but also on the robustness of the photogrammetric network and the geometric configuration of the survey (Sanz-Ablanedo et al., 2020; Agüera-Vega et al., 2023). In UAS surveys, flight altitude represents one of the most sensitive parameters in this planning. In general terms, lower altitude flights tend to produce smaller GSD and higher levels of detail, favoring feature identification and model densification, while higher altitudes favor the coverage of larger areas with lower computational effort, which may be advantageous in productivity-oriented operations. This relationship between geometric quality and operational efficiency has been discussed in different application contexts, including ISPRS studies focused on the influence of altitude, block geometry, and georeferencing strategy on the final accuracy of products (Abou Chakra et al., 2020).

Despite recent advances, there are still gaps regarding the integrated quantification of gains and limitations associated with different flight altitudes under controlled conditions, especially in urban environments. Part of the literature emphasizes improvements in accuracy with more robust blocks, the use of cross flights or oblique images, while another part highlights the importance of RTK/PPK georeferencing and the minimum distribution of GCPs for block stabilization. However, these studies do not always simultaneously evaluate external accuracy, data density, and operational efficiency of missions performed with comparable geometries and consistent processing parameters (Gerke and Przybilla, 2016; Teppati Losè et al., 2020; Agüera-Vega et al., 2023).

Therefore, this study proposes to compare two nadiral photogrammetric surveys carried out in an urban area, mainly differentiated by flight altitude, with overlap and processing parameters kept constant. The objective is to analyze how variations in altitude, and consequently in GSD, affect data density, block geometric quality, and the positional accuracy of the generated products, as well as to discuss the trade-off between detail and operational efficiency. Thus, this study aims to contribute to the definition of more appropriate acquisition strategies for different purposes in urban mapping using UAS. Additionally, it is expected to advance the understanding of the factors that control the quality of products generated by UAS, contributing to the development of more efficient and technically grounded guidelines for planning photogrammetric missions in urban environments.

2. Methology

Two photogrammetric surveys were carried out using RGB sensors with similar characteristics: one with the Mavic 3 Enterprise (M3E_12.3) and the other with the Matrice 4 Enterprise (M4E_12.3), both with a resolution of 5280 × 3956 pixels.

The flights were configured as follows: (i) a flight at 60 m altitude (low), with a Ground Sample Distance (GSD) of approximately 1.7 cm, totaling 426 images; (ii) a flight at 120 m altitude (high), resulting in a GSD of 3.29 cm, with 116 images. Both surveys were conducted with the camera in nadir position, maintaining 80% forward overlap and 70% side overlap.

The ground control network was established using a Polaris S100 GNSS receiver, operating in real-time kinematic (RTK) mode via the NTRIP correction service (RBMC-IP/IBGE). Positioning was performed in relative mode, with ambiguity-fixed solutions for all control and check points, ensuring centimeter-level accuracy (Cintra et al., 2011; Weber et al., 2005).

The baseline length between the rover and the reference station (PERC – Recife) was approximately 700 m, a condition considered highly favorable for minimizing the propagation of atmospheric and orbital errors, as well as improving positioning accuracy (Odolinski et al., 2015; Reddy, 2018).

For the development of this study, a total of 22 photo-identifiable and pre-signalized points were selected and surveyed within the study area, considering their visibility and stability, and ensuring they were visible in both flight processings. Subsequently, 14 targets were consolidated after quality assessment and divided into two independent sets: 9 Ground Control Points (GCPs), used in the bundle adjustment, and 5 Check Points (CPs), used exclusively for external accuracy evaluation. This separation ensures an unbiased assessment of the photogrammetric model accuracy and is widely recommended in UAV studies (James et al., 2017; James and Robson, 2012; Sanz-Ablanedo et al., 2020).

To evaluate the reliability of GNSS observations, positioning data were recorded in NMEA format during field acquisition. Although this format does not contain raw observations suitable for post-processing, it provides relevant information about solution quality, including its status (fixed, float, or standalone) and the temporal variability of the estimated coordinates (Hussein, 2016; Ilieva, 2021).

The trajectories were analyzed in QGIS (QGIS Development Team, 2025), using the LFTools plugin version 2.9.3 (França, 2026). Initially, the NMEA to Layer tool was used to convert the logs into a georeferenced point layer, allowing visualization of positional dispersion. Subsequently, the Nearest Points tool was applied to compute spatial discrepancies between positions derived from NMEA and the final coordinates obtained with fixed RTK solutions, enabling the estimation of statistical metrics such as standard deviation.

This procedure allowed the identification of solution quality patterns, where fixed solutions indicate resolved carrier-phase ambiguities and higher accuracy, while float and standalone solutions represent degradation in positioning accuracy (Zhu et al., 2018). The nominal accuracy assigned to each Ground Control Point (GCP) in the photogrammetric processing was 0.02 m in both planimetry and altimetry, consistent with the expected accuracy for RTK GNSS surveys under favorable conditions (Odolinski et al., 2015; Sanz-Ablanedo et al., 2020).

A total of 14 targets were materialized and measured in the test area, divided into two sets: fourteen GCPs and eight Check Points (CPs). The same points were used in the processing of both flights, and the influence of their spatial distribution was not evaluated in this study. According to Figure 1, float and standalone solutions occurred predominantly in obstructed environments, such as areas with vegetation or nearby structures, where multipath effects and signal blockage compromise GNSS performance (Tonkin and Midgley, 2016; Zhu et al., 2018).

Nevertheless, all GCPs and CPs used in the photogrammetric processing were collected under fixed solution conditions, ensuring high positional reliability.

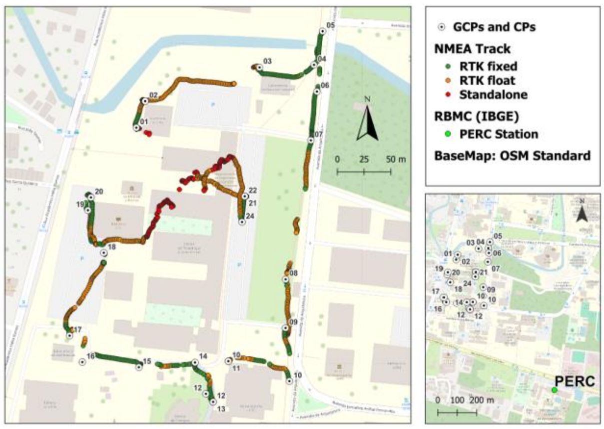

Figure 1: GCP and CP distribution with GNSS NMEA trajectory classified by solution status (RTK fixed, float, and standalone), including the RBMC (PERC) reference station location.

Image processing was carried out using the Agisoft Metashape software, adopting the default High and Aggressive configuration, consisting of: camera self-calibration, image alignment, generation of the sparse point cloud, insertion and measurement of control and check points, optimization of the bundle adjustment, and finally, generation of the dense point cloud, DEM (Digital Elevation Model), and orthomosaic, followed by the processing report.

It is noteworthy the application of altimetric correction for converting ellipsoidal (GNSS) altitudes into orthometric (physical) altitudes, using a value of +5.66 m, according to the geoid model for altitude conversion hgeoHNOR2020 adopted in Brazil (IBGE, 2023).

https://doi.org/10.5194/isprs-archives-XLIX-B1-2026-347-2026

3. Results and Discussion

In the surveys, the same sensor and the same lateral and longitudinal overlap were used. For processing, the same parameters were configured to obtain the products, as well as the same Ground Control Points (GCPs) and Check Points (CPs). The only independent variable was the flight altitude, with one flight conducted at 120 meters and the other at 60 meters, allowing the comparison of the influence of the Ground Sample Distance (GSD) on accuracy and data density.

Regarding the sensors used, both flights employed RGB cameras with the same resolution (5280 × 3956 pixels), consisting of equipment that is easily accessible in the context of mapping with commercial UAVs, which reinforces the practical applicability of the obtained results.

After processing each flight, the results presented in Table 1 were obtained. In the initial stage, point quality reports and positional error estimates were generated. In order to improve processing accuracy, points with positional errors greater than 1 meter in the X, Y, and Z coordinates were removed, resulting in the elimination of five collected points. In total, 13 points remained, consisting of 8 GCPs and 5 CPs, some being photo-identifiable and others pre-signalized. The use of 8 to 10 GCPs for processing provides reliability and stabilization of pronounced errors (Zhong et al., 2025), which enabled the removal of points with higher

The results obtained in this study corroborate the theoretical expectation that flight altitude is a key factor modulating geometric quality and data density. Flight 1 (M3E), operated at a lower altitude of approximately 60 m, achieved a GSD of 1.56 cm, while Flight 2 (M4E), at about 120 m, resulted in a resolution of 3.11 cm. This variation, proportional to altitude, produced a numerically superior model in Flight 1, mainly due to its higher spatial resolution (GSD) and the greater number of images acquired.

The results highlight two distinct mapping strategies: one prioritizing detail and the other productivity. Flight 1 achieved higher density and geometric detail, while Flight 2 focused on operational efficiency, covering a larger area (19.0831 ha) with only 116 images, compared to 426 images in Flight 1. This configuration characterizes Flight 2 as more efficient from an operational standpoint, reducing field acquisition time, data volume, and computational effort required for processing

Even under equivalent processing configurations, the observed differences demonstrate that the final quality of the products is directly conditioned by the characteristics of the flight plan and, consequently, by the input data. In terms of density, Flight 1 generated 3,132,168 3D points, while Flight 2 produced 852,200 points, a difference explained by the greater effective overlap and geometric redundancy provided by the higher number of images at lower altitude. This reinforces that, even with standardized processing, point cloud density is strongly dependent on GSD and the number of acquired images.

Parameter	Flight 1 (M3E)	Flight 2 (M4E)
Camera Model	M3E_12.3_5280×3956	M4E_12.3_5280×3956
GSD (Ground Sample Distance)	1.56 cm	3.11 cm
Flight Altitude (Estimated)	60 m	120 m
Images	420	116
Covered Area	15.4280 ha	19.46 ha
Calibrated Images	420 / 426 (98.7%)	116 / 116 (100%)
Tie Points	367,525	90,979
Processing Template	3D Maps (Full Scale)	3D Maps (Full Scale)
Projections	1,564,013	461,181
Global Reprojection Error	0.776 pix	0.804 pix
Markers	14	14
3D Points (BBA)	3,132,168	852,200
GCPs Used (3D)	9	8
Check Points (CPs)	5	5
RMSE CPs (Horizontal - X)	4.56709 cm	7.1715 cm
RMSE CPs (Horizontal - Y)	3.4354 cm	5.60077 cm
RMSE CPs (Vertical - Z)	3.21466 cm	3.98559 cm
Dense Point Cloud	212,879,281	67,884,583
Point Density	379 points/m²	97.7 points/m²

Table 1. Acquisition parameters and processing metrics of the photogrammetric flights (Flight 1 and Flight 2), including sensor characteristics, spatial resolution (GSD), flight altitude, covered area, number of calibrated images, processing configuration, and statistics derived from bundle block adjustment (BBA), such as keypoints, matches, and 3D point density.

On the other hand, although less operationally efficient, Flight 1 stands out for its level of detail, better spatial definition, and greater ability to represent even small terrain variations, making it more suitable for applications requiring high geometric accuracy and detailed representation. The use of a coarser scale in Flight 2 resulted in a higher reprojection error of 1.973 pixels, whereas in Flight 1 it was 0.920 pixels, indicating a more consistent mathematical adjustment in numerical terms, which results in better spatial resolution for the lower-altitude flight.

The dispersion of residual values of photogrammetric coordinates showed different behavior between the flights, with better planimetric and altimetric performance in Flight 1, with X, Y, and Z values of 0.016 m, 0.008 m, and 0.008 m, respectively. In Flight 2, these residuals were 0.023 m, 0.062 m, and 0.054 m for X, Y, and Z, respectively. This behavior indicates that higher spatial resolution leads to better positional quality of the photogrammetric product.

In this context, the use of natural control points proved to be a limiting factor regarding their spatial distribution in the field; however, it was still possible to obtain satisfactory values proportional to flight altitude. In general, it can be concluded that, although the processing was conducted under the same conditions, the differences observed in the final products are essentially due to the adopted flight plan, especially altitude and image density, highlighting Flight 1 for its geometric quality and Flight 2 for its operational efficiency.

4. Conclusion

However, the study demonstrated that flight altitude is a relevant factor in the quality of photogrammetric products, directly influencing spatial resolution, point cloud density, and the geometric and positional stability of the generated models. The photogrammetric products obtained from the processing of Flight 1 and Flight 2 highlight the importance of detailed flight planning to achieve the desired product (scale, spatial resolution, etc.). Despite the differences in product quality, depending on the intended application, Flight 2 presents advantages in terms of acquisition and processing time, which may influence its selection. Thus, the choice of flight altitude should be guided by the objectives of the survey: applications that require high detail and vertical accuracy benefit from lower-altitude flights, while large-scale surveys prioritize higher-altitude flights. The use of photo-identifiable points facilitated and accelerated data acquisition in the field; however, for future studies, it is recommended to use a minimum number of pre-signalized targets, as suggested by the ASPRS (2024) guidelines. Additionally, the incorporation of cross-strips and oblique imagery is recommended to further improve the understanding of the interaction between spatial resolution and acquisition geometry in the accuracy of the models.

References

Abou Chakra, C., Somma, J., Gascoin, S., Fanise, P., Drapeau, L., 2020. Impact of flight altitude on unmanned aerial photogrammetric survey of snow height on Mount Lebanon. *Int. Arch. Photogramm. Remote Sens. Spatial Inf. Sci.* XLIII-B2-2020, 119–125. doi.org/10.5194/isprs-archives-XLIII-B2-2020-119-2020.

Agüera-Vega, F., Carvajal-Ramírez, F., Martínez-Carricondo, P., 2023. Enhancing UAV-SfM 3D models accuracy of complex infrastructure with low-cost oblique imaging and optimized GCP configuration. *Int. Arch. Photogramm. Remote Sens. Spatial Inf. Sci.* XLVIII-M-2-2023, 51–58. doi.org/10.5194/isprs-archives-XLVIII-M-2-2023-51-2023.

Cintra, J.P., Nero, M.A., Rodrigues, D., 2011. GNSS/NTRIP service and technique: accuracy tests. *Bol. Ciênc. Geod.* 17(2), 257–271. doi.org/10.1590/S1982-21702011000200006.

França, L.S., 2026. LFTools: plugin para processamento de dados geoespaciais em QGIS, Version 2.9.3. Universidade Federal de Pernambuco, Recife.

Gerke, M., Przybilla, H.-J., 2016. Accuracy analysis of photogrammetric UAV image blocks: influence of onboard RTK-GNSS and cross flight patterns. *Photogramm. Fernerkund. Geoinf.* 2016(1), 17–30. doi.org/10.1127/pfg/2016/0284.

Gomes, A.D.A.R., Silva, B.N., Barros, B.A., Giri, F.B., Nunes, J.C.B., Oliveira, M.P., Rodrigues, D.S., 2024. O uso de drones para mapeamento topográfico. *Rev. Gestão e Secretariado* 15(5), e3799.

Hussein, Z.E., 2016. Improving the accuracy of handheld GPS receivers based on NMEA file generating and least squares adjustment. *J. Eng.* 22, 162–174. doi.org/10.31026/j.eng.2016.05.11.

IBGE, 2023. Modelo hgeoHNOR2020 para conversão de altitudes geométricas em altitudes normais, 2nd ed. IBGE, Coordenação de Geodésia, Rio de Janeiro.

Ilieva, T., 2021. Development of a web-based system for GNSS data tracking and applying corrections in GIS environment. *Int. Multidiscip. Sci. GeoConf. SGEM Proc.*, 239–246. doi.org/10.5593/sgem2021/2.1/s08.32.

James, M.R., Robson, S., 2012. Straightforward reconstruction of 3D surfaces and topography with a camera: accuracy and geoscience application. *J. Geophys. Res.* 117, 2011JF002289. doi.org/10.1029/2011JF002289.

James, M.R., Robson, S., Smith, M.W., 2017. 3-D uncertainty-based topographic change detection with structure-from-motion photogrammetry. *Earth Surf. Process. Landf.* 42, 1769–1788. doi.org/10.1002/esp.4125.

Nikolakopoulos, K.G., Kyriou, A., Koukouvelas, I.K., 2022. Developing a guideline of unmanned aerial vehicle’s acquisition geometry for landslide mapping and monitoring. *Appl. Sci.* 12(9), 4598.

Niu, Z., Wang, Y., Zhang, X., Li, J., 2024. Accuracy assessment of UAV photogrammetry system with RTK/Network RTK in built environments. *ISPRS Ann. Photogramm. Remote Sens. Spatial Inf. Sci.* X-1-2024, 169–176. doi.org/10.5194/isprs-annals-X-1-2024-169-2024.

Odolinski, R., Teunissen, P.J.G., Odijk, D., 2015. Combined GPS + BDS for short to long baseline RTK positioning. *Meas. Sci. Technol.* 26, 045801. doi.org/10.1088/0957-0233/26/4/045801.

Reddy, G.P.O., 2018. Global positioning system: principles and applications. In: Reddy, G.P.O., Singh, S.K. (Eds.), *Geospatial Technologies in Land Resources Mapping, Monitoring and Management*. Springer, Cham, pp. 63–74. doi.org/10.1007/978-3-319-78711-4_4.

Sanz-Ablanedo, E., Chandler, J.H., Ballesteros-Pérez, P., Rodríguez-Pérez, J.R., 2020. Reducing systematic dome errors in digital elevation models through better UAV flight design. *Earth Surf. Process. Landf.* 45, 2134–2147. doi.org/10.1002/esp.4871.

Silva, L.S., Zanoni, V.A.G., Pazos, V.C., Santos, L.M.A., Jucá, T.R.P., 2022. Fotogrametria com imagens adquiridas com drones.

Teppati Losè, L., Chiabrando, F., Tonolo, F.G., 2020. Are measured ground control points still required in UAV-based large-scale mapping? Assessing positional accuracy of an RTK multi-rotor platform. *Int. Arch. Photogramm. Remote Sens. Spatial Inf. Sci.* XLIII-B1-2020, 507–514. doi.org/10.5194/isprs-archives-XLIII-B1-2020-507-2020.

Tonkin, T., Midgley, N., 2016. Ground-control networks for image-based surface reconstruction. *Remote Sens.* 8, 786. doi.org/10.3390/rs8090786.

Weber, G., Dettmering, D., Gebhard, H., 2005. Networked transport of RTCM via internet protocol (NTRIP). In: Sansò, F. (Ed.), *A Window on the Future of Geodesy*. Springer, Berlin/Heidelberg, pp. 60–64. doi.org/10.1007/3-540-27432-4_11.

Zhong, H., Duan, Y., Tao, P., Zhang, Z., 2025. Influence of ground control point reliability and distribution on UAV photogrammetric 3D mapping accuracy. *Geo-spatial Inf. Sci.* 28(5), 1998–2018. doi.org/10.1080/10095020.2025.2451204.

Zhu, N., Marais, J., Betaille, D., Berbineau, M., 2018. GNSS position integrity in urban environments: a review of literature. *IEEE Trans. Intell. Transp. Syst.* 19, 2762–2778. doi.org/10.1109/TITS.2017.2766768.